CORA Cork Open Research Archive
Cartlann Taighde Oscailte Chorcaí

Title	Distributed fibre optic sensing of a deep excavation adjacent to pre-existing tunnels
Authors	Li, Zili;Soga, Kenichi;Kechavarzi, Cedric
Publication date	2018-09-28
Original Citation	Li, Z., Soga, K. and Kechavarzi, C. (2018) 'Distributed fibre optic sensing of a deep excavation adjacent to pre-existing tunnels', Géotechnique Letters, 8(3), pp. 171-177. doi: 10.1680/jgele.18.00031
Type of publication	Article (peer-reviewed)
Link to publisher's version	https://www.icevirtuallibrary.com/doi/abs/10.1680/jgele.18.00031 - 10.1680/jgele.18.00031
Rights	© 2018, ICE Publishing. All rights reserved. This document is the Accepted Manuscript version of a Published Work that appeared in final form in Géotechnique Letters 8(3), pp. 171-177. To access the final edited and published work see https://doi.org/10.1680/jgele.18.00031
Download date	2026-10-30 10:41:35
Item downloaded from	https://hdl.handle.net/10468/7837

UCC
University College Cork, Ireland
Coláiste na hOllscoile Corcaigh

Main Text (Include word count on title page)
Click here to download Main Text (Include word count on title page) R3 distributed fibre optic sensing of Paddington

Distributed Fibre Optic Sensing of a Deep Excavation Adjacent to Pre-existing Tunnels

Zili Li[1], Kenichi Soga[2] , Cedric Kechavarzi[3]

1 *Lecturer, Civil & Environmental Engineering, University College Cork, Cork, Republic of Ireland; formerly University of Cambridge, Cambridge, UK*
E-mail: zili.li@ucc.ie
2 *Professor, Civil and Environmental Engineering, University of California, Berkeley, USA; formerly University of Cambridge, Cambridge, UK*
E-mail: soga@berkeley.edu
3 *Senior Research Associate, Cambridge Centre for Smart Infrastructure and Construction, University of Cambridge, Cambridge, UK*
E-mail: ck209@eng.cam.ac.uk

ABSTRACT

This paper investigated a diaphragm wall behaviour due to deep excavation at Paddington tunnel station site in London clay. The Paddington site was the only train station in the Crossrail project constructed using a top-down excavation, and it provided the opportunity to evaluate the effect of a pre-existing tunnel on D-wall behavior using distributed fibre optic sensing (DFOS) for the first time. Distributed fibre optic cables were embedded in diaphragm wall panels to monitor the changes in strain conditions during three key stages of construction; tunnel passage, concourse excavation and base excavation. After station construction, relevant finite element analysis was conducted to evaluate the D-wall performance during excavation, and the computed results were compared against the field measurements recorded by embedded DFOS in the D-wall as well as the ground inclinometers. The DFOS measurements depicted the D-wall behaviour in agreement with the conventional inclinometer method and finite element results, demonstrating its feasibility in monitoring underground earth retaining infrastructure. A comparison between the diaphragm wall behaviour with pre-existing tunnels at Paddington site and that of the same wall without tunnel allows providing some guidance for the design and construction of retaining structures adjacent to pre-existing tunnels.

KEYWORDS: *Distributed fibre optic sensing, Diaphragm wall, wall-tunnel interaction, Top-down excavation, Pre-existing tunnel*

Word count: 3046

1. INTRODUCTION

Underground construction in congested urban environment has been increasingly challenging over the recent decades and necessitates appropriate field monitoring at construction site. Recently, distributed fibre optic sensing (DFOS) is emerging as an innovative monitoring tool for continuous measurement of strain development in civil infrastructures in comparison to conventional discrete point sensors (e.g. vibrating wire strain gauges and ground

inclinometers). In the monitored structure, a fibre optic strain cable is usually instrumented along a reinforcement bar to obtain the strain distribution, along with a standard telecom cable for temperature compensation (Mohamad, 2008). At one end of the cables, an analyzer (e.g. Brillouin optical time domain reflectometry (BOTDR)) launches an optical pulse and subsequently measures the backscattered light launched, which is linearly proportional to the applied strain (Horiguchi et al., 1989).

As a pioneer, Klar et al. (2006) attempted to employ distributed optical fibres in pile foundations and obtained a complete pile-soil interaction profile more comprehensive than conventional discrete point measuring methods (e.g. strain gauges). Mohamad et al. (2011) extended the application of fibre optic sensing to monitor the strain and deflection development along a secant piled wall for a deep excavation, and the fibre optic measurements showed good agreement with the field data collected by inclinometers nearby. Later, Schwamb et al. (2014) instrumented fibre optic cables on 84 m deep diaphragm wall (D-wall) panels of Abbey Mills shaft to monitor the D-wall performance due to excavation and the measured mechanical strains of the wall in chalk was found to exceed the design predictions. In practice, DFOS has been adopted to some geotechnical infrastructure (Janmonta et al., 2008; Shi et al., 2003; Hauswirth et al., 2014), but obstacles still remain on the road for promoting this innovative technology to wider civil engineering applications (Pei et al, 2014); For example, sophisticated cable instrumentation workmanship shall be accumulated from many more demonstration cases in a wider range of geotechnical fields (e.g. diaphragm wall for deep excavation). The conversion of collected raw optic data to mechanical strain has to go through a series of processes, including time shift, frequency shift, temperature compensation and etc., whilst the development of professional algorithm and associated software for optic data processing is still underway.

Deep excavation in congested urban environment may inevitably have an impact on adjacent infrastructure, and as such diaphragm walls (D-wall) along with top-down excavation method has been widely adopted to control the ground disturbance (e.g. Ou et al., 1998; Finno, 2008; Kung, 2009; Chang et al., 2001). It is common in big cities that a new deep basement can only be constructed adjacent to pre-existing tunnels, and their interaction behaviour may be rather complicated. Shi et al. (2015) conducted both centrifuge modelling and numerical analysis to investigate the basement-tunnel interaction in two typical configurations: tunnel beneath a basement and tunnel at the side of a basement. Results show that tunnel located directly beneath a basement elongated due to stress relief from the basement excavation, whereas the tunnel distorted if located at the side of the basement. Similar interaction mechanisms were also predicted by semi-analytical method and analytical solution for quick estimation (Zhang et al. (2013a) and Zhang et al. (2013b)). Previous efforts mainly focused on the impact of deep excavation

on adjacent tunnels, whereas little attention was paid on the effect of a pre-existing tunnel on the D-wall behaviour. The pre-existing tunnel alters ground environment and boundary conditions at the excavation site, and therefore may lead to special deflection D-wall mode and ground displacement different from common excavation cases without tunnel.

This paper investigated the D-wall behaviour due to deep excavation at Paddington train station site in London clay. The new Paddington station was the only train station in London's Crossrail project constructed using a top-down excavation method framed with diaphragm walls. At this site, two tunnels were excavated through the station and later demolished during the station construction. The D-wall was instrumented with fibre optic cables and the ground displacement was monitored by inclinometers. In addition, relevant finite element analysis was conducted after station construction to evaluate the D-wall performance during excavation against the field measurements. Results revealed the effect of a pre-existing tunnel on D-wall behaviour using fibre optic cables for the first time, and confirmed that the ground surface can be well controlled using top-down excavation method in London clay.

2. FIELD MEASUREMENTS

2.1. CONSTRUCTION SITE

The Paddington train station site is almost rectangular: 262 m long, 23 m wide and 19 m deep (see Figure 1a&b). This station box is framed with diaphragm wall panels, and most of which are 1.2m thick, 3.4m wide and 38m long. The D-wall is connected with four slabs along the depth from top to bottom: roof slab, intermediate slab, concourse slab and base slab (see Figure 1c). Between the D-walls, two tunnels with a diameter of 7m were excavated along northwest-southeast direction, and the closer one was only 1.5m away from the D-wall.

The site construction went through three stages: tunnel passage, concourse excavation, base excavation as shown in Figure 1. Prior to the first tunnelling stage, the diaphragm wall panels were constructed at four corners of the station box. Tunnel boring machine then excavated through the Paddington site and the induced ground displacement was monitored by a group of inclinometers. For example, one inclinometer A15 was deployed 1.7m away from the D-wall section as marked in Figure 1b. The remaining D-wall panels were constructed afterwards, one of which was embedded with distributed fibre optic cables (DFOS) as marked in Figure 1b. A roof slab near the ground surface was cast thereafter, leaving a hole to facilitate the basement excavation underneath. Once the excavation reached the half of the concourse depth, a line of temporary props was installed between the D-walls to support the subsequent excavation down to the concourse depth; those props were then removed after the construction of the concourse slab. In the final base excavation stage, soil under the concourse slab was excavated to the base depth by demolishing the pre-existing tunnel halfway and eventually completed by the casting of the

base slab.

2.2. DISTRIBUTED FIBRE OPTIC SENSING

At the site, the distributed fibre optic cables were instrumented in a D-wall panel S56 adjacent to an inclinometer borehole for comparison as shown in Figure 1b. Based upon previous site experience, the cables were installed along the side face of the D-wall (see Figure 2a & b) instead of the front face immediately next to the excavation face as to reduce the risk of cable damage (Figure 2c). Fibre optic cables were instrumented along the reinforcement bars at two locations: one is on excavation side and the other is on soil side, and the spacing distance in between is 1m as illustrated in Figure 2b. Two types of optical fibre cables were installed: 1) Fujikura reinforced ribbon cable for strain sensing (strain cable) for both mechanical strain and thermal strain; 2) standard telecommunication cable for thermal strain only (temperature cable) since the presence of a gel layer in the cable tube eliminates mechanical strain in the fibre core. In the monitored D-wall panel, the mechanical strain due to excavation is derived from the strain cable measurements after temperature compensation using the temperature cable.

Figure 3 shows that the derivation of D-wall deflection from the strains measurements at soil side and excavation side, respectively. The difference between the two strain readings over the spacing distance gives the incremental curvature $\Delta\kappa$ as shown in Equation 1. Along the depth of the D-wall, z, the incremental gradient profile $\Delta\varphi$ and lateral displacement Δu can derived by integration from Equation 2 & 3, respectively:

$$\Delta\kappa = \frac{1}{d}\left(\Delta\varepsilon_s - \Delta\varepsilon_e\right) \quad (1)$$

$$\Delta\varphi = \int \Delta\kappa dz + A \quad (2)$$

$$\Delta u = \int \Delta\varphi dz + B \quad (3)$$

Where $\Delta\kappa$ is the incremental curvature over the thickness of the wall. $\Delta\varepsilon_s$ is the incremental mechanical strain on the soil side and $\Delta\varepsilon_e$ is the incremental mechanical strain on the excavation side. d is the spacing distance between the strain cables on the soil and excavation sides. $\Delta\varphi$ and Δu are the incremental gradient and lateral displacement, respectively. Their magnitude is influenced by the constants A, B: initial gradient and lateral displacement, respectively, which can be determined by other field measurements (e.g. inclinometers) or assumed boundary conditions. In this study, the values of constant A (initial gradient) and constant B (initial lateral displacement) were established at the top of the fibre optic cables based upon inclinometer data obtained at the intermediate slab level.

Conventionally, tensile strain in fibre optic sensing is denoted by positive value, whilst compressive strain is negative (Mohamad et al., 2011). If the incremental mechanical bending strain is positive (i.e. $\Delta\varepsilon_s - \Delta\varepsilon_e > 0$), the D-wall is under positive bending and bends towards the soil side. In contrast, the D-wall bends to the excavation side subject to negative bending moment if $\Delta\varepsilon_s - \Delta\varepsilon_e < 0$. The magnitude of bending moment is calculated by the relationship of $M = \kappa EI$, where κ is the curvature as mentioned earlier and *EI* is the flexural rigidity of the wall. The wall flexural stiffness (*EI*) was assumed as $0.7E_oI$ during station construction, where the short-term Young's modulus of uncracked concrete, E_o, was chosen as 28 GPa according to CIRIA C580 Report (Gaba et al. 2003).

In practice, DFOS reading is usually taken at each construction stage and the difference between DFOS readings is the incremental strain development between two stages, whilst the influence of concrete curing & shrinkage on the incremental strain development can be eliminated. In this project, the fibre optic data was taken at every 5 cm along the cable by an analyzer BOTDR, and each reading represented a weighted average of strain along approximately 0.5m gauge length. If a considerable crack occurs at a location, the accuracy of the optic reading nearby within the spatial resolution (±0.5m) may be compromised, whilst a huge spike will appear in the fibre optic data curve. In this Paddington project, there was no big spike detected in the field data curve, suggesting few substantial cracks and acceptable accuracy of the DFOS data.

3. FINITE ELEMENT ANALYSIS AND DISCUSSION

3.1 FINITE ELEMENT MODEL

In this study, a finite element analysis was conducted after station construction to evaluate the D-wall behaviour at Paddington site using ABAQUS software package. Since the station is long and narrow (262m in length and 23m in width), a 2D plane strain condition was considered in the modelling of the DFOS monitored D-wall panel cross section as shown in Figure 4. The vertical soil profile at the site is as follows: (a) Made Ground (0–3 m), (b) Terrace Gravel (3–6.5 m), and (c) London Clay (6.5–65 m) (d) Lambeth Group Clay (below 65m). Made Ground and Terrace Sand were modelled as linear elastic-perfectly plastic material with Mohr-Coulomb failure criterion, whereas London Clay and Lambeth Group were modelled using an advanced non-linear elasto-plastic critical state soil model (Wongsaroj, 2007; Laver, 2010). Table 1 & 2 list soil parameters adopted in the FE model based upon

characteristic soil properties suggested by Crossrail Ltd. (2011 and 2015). Due to lack of comprehensive lab test at Paddington site, some material properties of the advanced critical state model for London clay were assumed as typical values following Laver (2010). In particular, the parameters of small strain stiffness C_b and soil stiffness degradation ω_s were adjusted as to give the same characteristic soil properties (e.g. Young modulus and undrained shear strength) in Crossrail Ltd. (2011 and 2015). At the top of London clay, the mean effective preconsolidation pressure was assumed to be 900 kPa and increases linearly at 10 kPa /m along the depth. This gave an overconsolidation ratio from 4.5 to 11 along the depth of the D-wall in line with typical range between 4.3 ~ 12 for London clay Unit A & B as suggested by Gasparre (2005). The soil layer of Lambeth Group is far below the base slab level, and therefore, for simplicity, the material properties were assumed the same as the typical values given by Laver (2010).

Most part of the station was constructed in the low permeable London clay and therefore was assumed in an undrained condition, whilst the D-wall and slabs were modelled explicitly using 2D elements. The top boundary of the FE model was set to be free, whereas the vertical movements at the bottom boundary were fixed. At the sides, the horizontal movements were set to be zero. The water table was set to be 2m below the ground surface.

Based upon the same FE model, two scenarios were taken into account: one considered both tunnel passage and deep excavation according to the actual Paddington site construction, whereas the other only modelled the deep excavation step without a pre-existing tunnel, which represents a common deep construction scenario. The comparison between the two scenarios will evaluate the effect of a pre-existing tunnel on D-wall behaviour and ground movement nearby.

Paddington station construction was initially designed to be top-down with four levels: slabs, roof, intermediate, concourse and base slab, which were to be constructed one after the other. However, due to access constraints at the site, the intermediate slab was not constructed with the excavation but delayed until after completion of the concourse slab (Rutledge & Harrison, 2015), whilst the fibre optic data was then unable to be collected for the intermediate slab construction stage. In this study, the FE analysis evaluated the changes in strain and displacement conditions during three key stages of construction: tunnel passage, concourse and base excavation. The D-wall displacement due to tunnelling was recorded by inclinometers, and the magnitude was within 3 mm, which was much smaller that induced by deep excavation (e.g. more than 10 mm). Due to the construction requirement, fibre optic cables were only allowed to be instrumented in the D-wall panel after tunnel passage, and therefore only measured the strain changes in the D-wall at the subsequent two station excavation stages. For simplicity, the

following discussion on D-wall behaviour mainly focuses on the field measurements and FE results at two excavation stages: concourse excavation stage and base excavation stage.

3.2 RESULTS AND DISCUSSION

Figure 5 shows the development of the D-wall deflection due to concourse excavation from the roof slab to the concourse slab. The incremental D-wall deflection starts from zero at the roof slab and increases along the depth up to 14 mm near the pre-existing tunnel level. Due to the lateral ground resistance below the concourse slab, the D-wall gradually bends back to the soil side. The computed D-wall displacement from the FE simulation shows good agreement with the DFOS field measurements, while their magnitude is greater than the ground movement measured by the conventional inclinometers at a distance away from the D-wall panel as mentioned earlier.

To investigate the effect of a pre-existing tunnel on deep excavation, the Paddington site case with pre-existing tunnels was compared against the same excavation scenario without tunnel, and the D-wall deflections of the two scenarios are shown in Figure 5b. Compared with deep excavation scenario without tunnel, the presence of a pre-existing tunnel does not change the shape of D-wall deflection significantly except inducing slightly greater displacement of 1.6 mm at the tunnel level. Due to the pre-existing tunnel, the lateral ground resistance underneath the concourse slab is reduced to be less than that of the initial ground condition. After soil excavation, the pre-existing tunnel ovalizes vertically and therefore results in additional D-wall deflection in the horizontal direction. The FE model predicted an accumulated tunnel ovalisation of 0.35% after concourse excavation, which shows agreement with the measured ovalisation of around 0.31% derived from field data (Rutledge & Harrison, 2015).

Figure 6 shows the incremental D-wall bending strains induced by base excavation below the concourse slab. Above the intermediate slab, the D-wall bending strain is negligible due to the support of roof slabs and intermediate slabs during top-down excavation. Below the intermediate slab, the incremental bending strain increases up to 320 positive microstrains at the concourse slab near the pre-existing tunnel. The incremental bending then starts to decrease gradually to be negative along the depth up to -220 negative microstrains at the base level, and ends up to be negligible at the depth of 28m due to ground support below the base slab. The findings are generally in line with typical excavation-induced D-wall behaviour as confirmed by the results derived from the FE model.

Likewise, Figure 6b compares the D-wall deflection from excavation scenario without tunnel and Paddington site

scenario with pre-existing tunnels. There is little difference between the two scenarios above the concourse slab level due to the solid support of the slabs above. Below the concourse slab, the excavation scenario without tunnel excavates all the soil between concourse slab and base slab, whereas in the Paddington site scenario only the soil surrounding the pre-existing tunnel is removed. The more soil excavated in the excavation scenario without tunnel therefore induces greater horizontal deflection than the Paddington site scenario with a tunnel. Underneath the base slab, the maximum deflection of the excavation scenario without tunnel is 10.9 mm, which is 2.2 mm (i.e. 25%) more than the deflection of 8.7 mm at Paddington site scenario.

4. CONCLUSION

This study investigated the effect of a pre-existing tunnel on D-wall behaviour using distributed fibre optic cables for the first time. In addition, a 2D plane strain finite element analysis was conducted after the field measurements were recorded, and the computed results were then compared with the measurements. The main findings of this paper are given as follows:

- The DFOS measurements confirmed that the ground surface can be well controlled using top-down excavation method in London clay. The D-wall deflection derived from fibre optical data shows agreement with the conventional inclinometer method and finite element results, demonstrating the feasibility of DFOS in monitoring underground earth retaining infrastructure.
- At Paddington site, the D-wall displacement due to tunnel excavation was relatively small within 3m as recorded by inclinometers. The maximum incremental lateral displacement of 14 mm appears near the pre-existing tunnel level due to concourse excavation.
- The presence of pre-existing tunnels reduced the lateral ground resistance at Paddington site, and as such induced slightly greater incremental D-wall deflection than that of the same excavation scenario without tunnel at the concourse excavation stage.
- At the base excavation stage, there was less development of lateral ground displacement in Paddington site scenario than the excavation scenario without tunnel, since less volume of soil was excavated due to the pre-existing tunnels at Paddington station site.

AKCNOWLEDGEMENT

This work was supported by EPSRC (Innovation and Knowledge Centre for Smart Infrastructure and Construction (CSIC) - Collaborative Programme), UK and National Natural Science Foundation of China (No. 5170080836, No. 51608539 and No. 51508403). The authors would like to thank Andrew Davie at OTB Engineering, Njemile Faustin, Seda Torisu and some other colleagues for their kind assistance.

REFERENCES

ABAQUS Inc. (2010). ABAQUS User's Manual, Version 6.12. SIMULIA. www.simulia.com.

Chang, C.T., Sun, C.W., Duan, S.W. & Hwang, R.N. (2001). Response of a Taipei Rapid Transit System (TRTS) tunnel to adjacent excavation. *Tunn. Undergr. Sp. Technol.* **16**, No. 3, 151–158.

Crossrail Limited. (2011). C130 – Paddington Station, Geotechnical Design Report: Part 2, Geotechnical Design Summary Report. Document Number: C130-SWN-C2-RGN-B071-00004.

Crossrail Limited. (2015). Multi-Disciplinary Consultant Work Package 2, Paddington Station – Scheme Design Report, Volume 3 – Civil, Structural & Tunnel Engineering Report. Document Number: CR-SD-PAD-CE-RT-00002.

Finno, R.J. (2008). Analysis and numerical modeling of deep excavations 87-97 Geotechnical aspects of underground construction in soft ground. *Proceedings of the 6th International Symposium (IS-Shanghai 2008)*, Shanghai, China.

Gaba, A. R., Simpson, B., Powrie, W. & Beadman, D. R. (2003). CIRIA Rep. C580: Embedded retaining walls: Guidance for economic design. CIRIA, London.

Hauswirth, D., Puzrin, A.M., Carrera, A., Standing, J.R. & Wan, M.S.P. (2014). Use of fibre-optic sensors for simple assessment of ground surface displacement during tunnelling. *Géotechnique*. **64**, 837-842.

Horiguchi, T. & Tateda, M. (1989). BOTDA-nondestructive measurement of single-mode optical fiber attenuation characteristics using Brillouin interaction: theory, *J. Lightwave Technol*. **7**, No. 8, 1170−1176.

Janmonta, K., Uchimura, T., Amatya, B., Soga, K., Bennett, P., Lung, R. & Robertson, I. (2008). Fibre optics monitoring of clay cuttings and embankments along London's ring motorway. *Geocongress 2008: Characterization Monitoring and Modeling of Geosystems*, pp. 209–516.

Klar, A., Bennett, P. J., Soga, K., Mair, R. J., Tester, P., Fernie, R., St JOHN, H. D. & Torp-Peterson G. (2006). Distributed Strain Measurement for Pile Foundations. *Proceedings of the Institution of Civil Engineers - Geotechnical Engineering*. **159**, 135–144.

Kung, T. C. & Ou, C. Y. (2006). Prediction of surface settlement caused by excavation. In: Bakker, K. J., Broere, W., and Bezuijen, A. (eds.), *Proceedings of the 5th International Symposium TC28 on Geotechnical Aspects of Underground Construction in Soft Ground*, Taylor & Francis Group / Balkema, pp. 853–858.

Laver, R. (2010). Long-term behaviour of twin tunnels in London Clay. Ph.D. thesis, the University of Cambridge, Cambridge, UK.

Mohamad H. (2008). Distributed Optical Fibre Strain Sensing of Geotechnical Structures. PhD thesis, Department of Engineering, Cambridge University, UK.

Mohamad H., Bennett P., Soga K., Klar A. & Pellow A. (2011). Distributed optical fiber strain sensing in a secant piled wall, *J. Geotech. Geoenviron. Eng*. **137**, No. 12, 1236–1243.

Ou, C., Liao, J. & Lin H. (1998). Performance of diaphragm wall using top-down method. *J Geotech Geoenviron Eng*. **124**, No. 9, 798–808.

Pei, H., Teng, J., Yin, J. & Chen, R. (2014). A review of previous studies on the applications of optical fiber sensors in geotechnical health monitoring. *Measurement*. **58**, pp. 207–214.

Rutledge, H. & Harrison, S. (2015). Digging for monitoring gold: in-tunnel monitoring during the Crossrail Paddington Station box excavation. Crossrail Learning Legacy, ICE Publishing.

Schwamb, T. (2014). Performance Monitoring and Numerical Modelling of a Deep Circular Excavation. PhD thesis, Department of Engineering, Cambridge University, UK.

Shi, B., Xu, H.Z., Zhang, D., Ding, Y., Cui, H.L., Gao, J.Q. & Chen, B. (2003). A study on BOTDR application in monitoring deformation of a tunnel. *Proceedings 1st International Conference of Structural Health Monitoring and Intelligent Infrastructure*, Tokyo, Japan, pp. 1025–1030.

Shi, J., Ng, C.W.W. & Chen, Y. (2015). Three-dimensional numerical parametric study of the influence of basement excavation on existing tunnel. *Computers and Geotechnics*. **63**, 146–158.

Wongsaroj, J., Soga, K. & Mair, R. J. (2007). Modelling of long term ground response to tunnelling under St James' Park London. *Geotechnique*. **57**, pp. 75–90.

Zhang, J., Chen, J., Wang, J. & Zhu, Y. (2013a). Prediction of tunnel displacement induced by adjacent excavation in soft soil. *Tunnelling and Underground Space Technology*. **36**, 24–33

Zhang, Z., Huang, M. & Wang, W. (2013b). Evaluation of deformation response for adjacent tunnels due to soil unloading in excavation engineering. *Tunnelling and Underground Space Technology*. **38**, 244–253

List of Figures

Figure 1 Diaphragm wall excavation box at Paddington Station
(a) Photo of Paddington excavation site (Copyright Crossrail Ltd.)
(b) Schematic of the excavation (top view)
(c) Schematic of the excavation (side view)

Figure 2 Location of optical fibre instruments
(a) Fibre optic cables instrumented on the steel cage
(b) installation on the side face (c) installation on the front face

Figure 3 Derivation of D-wall deflection from strains measurements ε_s and ε_e along fibers at soil side and excavation side, respectively

Figure 4 Finite element model of Paddington station site
(a) FE results versus field measurements (b) The effect of the existing tunnel (tunnel deformation is not to scale)

Figure 5 Incremental lateral displacement along the D-wall due to concourse excavation
(a) FE results versus field measurements (b) The effect of the existing tunnel

Figure 6 Incremental bending strain along the D-wall due to base excavation

Figure 1a

Click here to download Figure Figure 1a.jpg

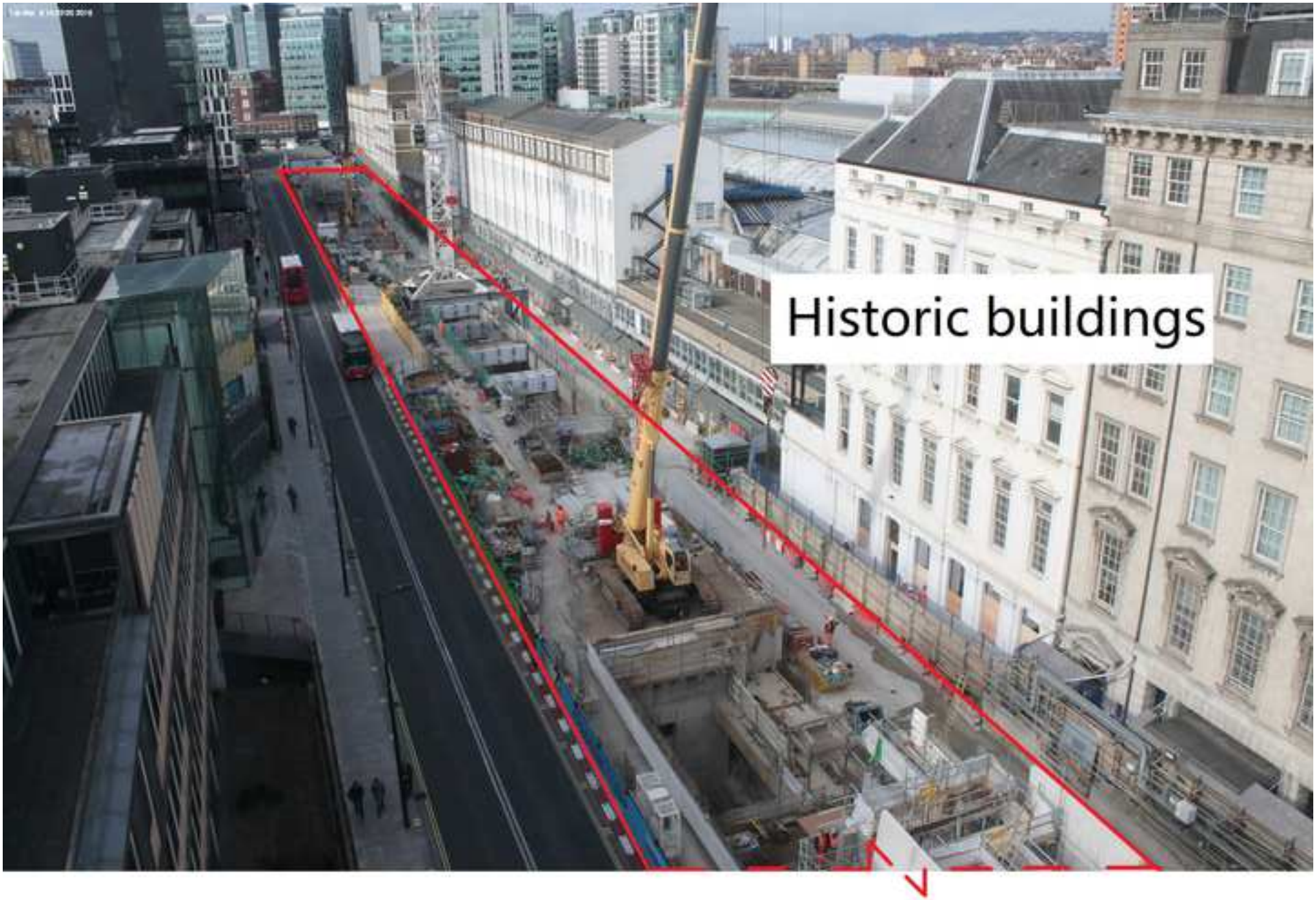
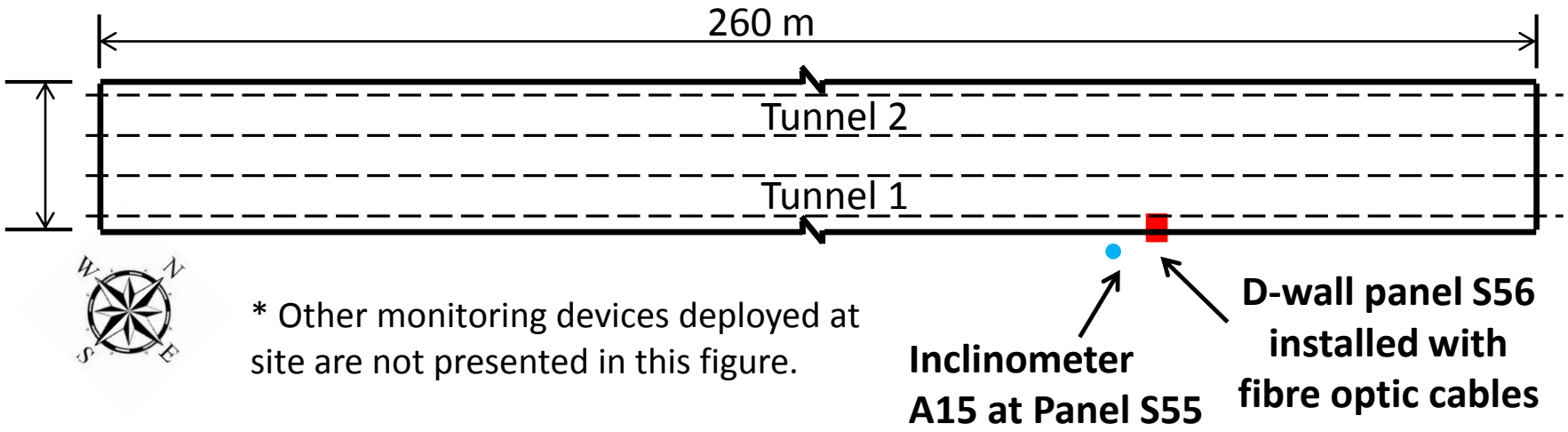


Figure 1b&c

Click here to download Figure Figure 1b&c.pptx



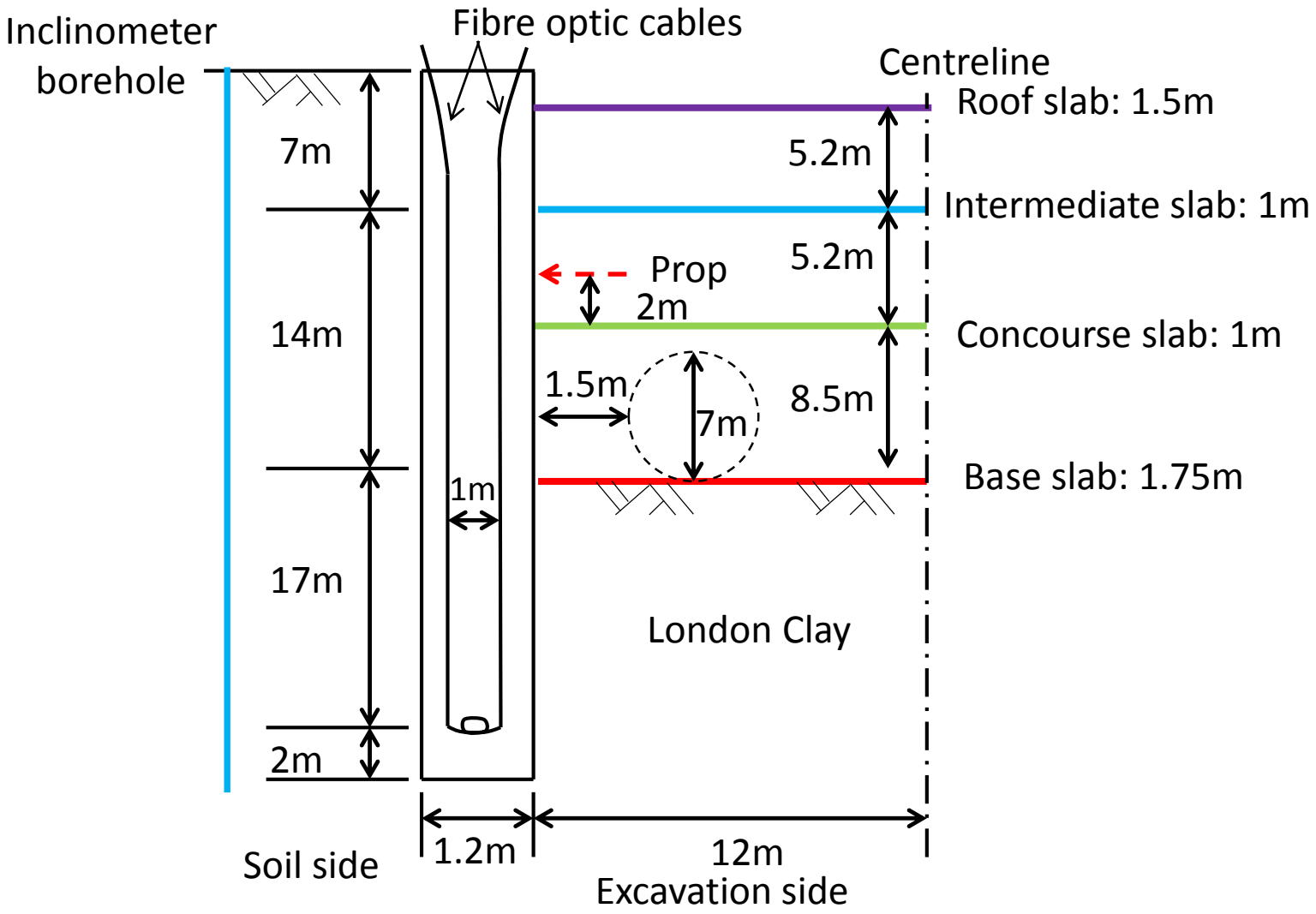

Inclinometer borehole
Fibre optic cables
Centreline
Roof slab: 1.5m
Intermediate slab: 1m
Concourse slab: 1m
Base slab: 1.75m
Prop
2m
7m
14m
17m
2m
1m
1.5m
7m
5.2m
5.2m
8.5m
London Clay
Soil side
1.2m
12m
Excavation side

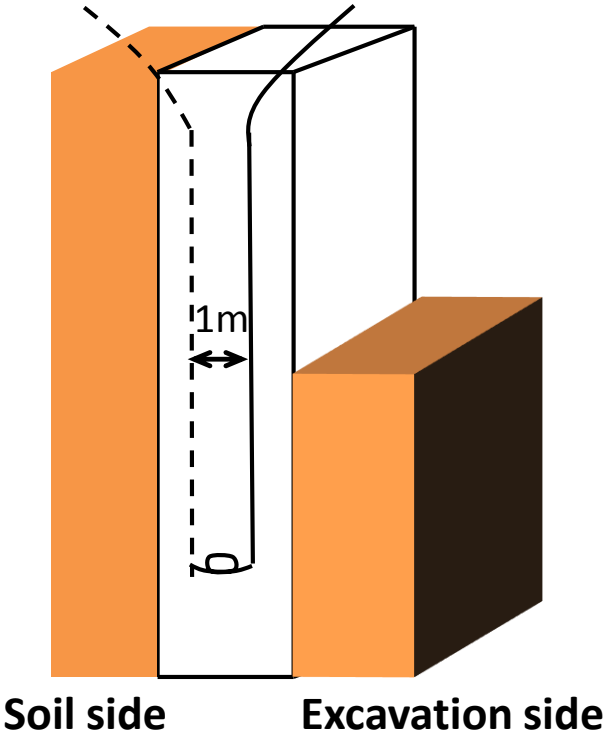
Figure 2a

Click here to download Figure Figure 2a.JPG



Figure 2b&c

Click here to download Figure Figure 2b&c.pptx



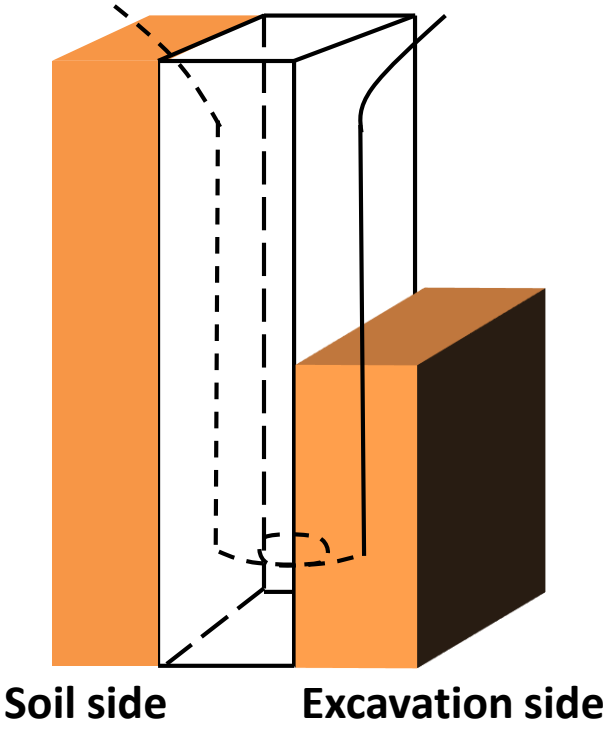


Figure 3

Click here to download Figure Figure 3.pptx

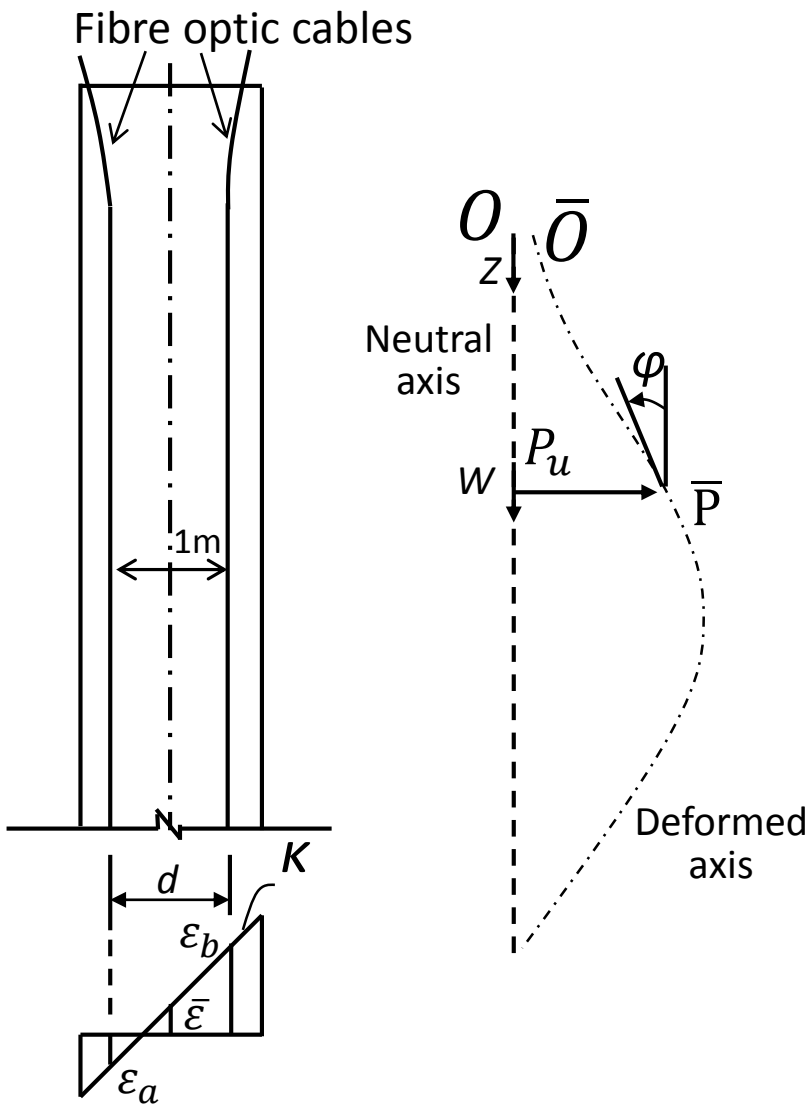


Figure 4

Click here to download Figure Figure 4.pptx

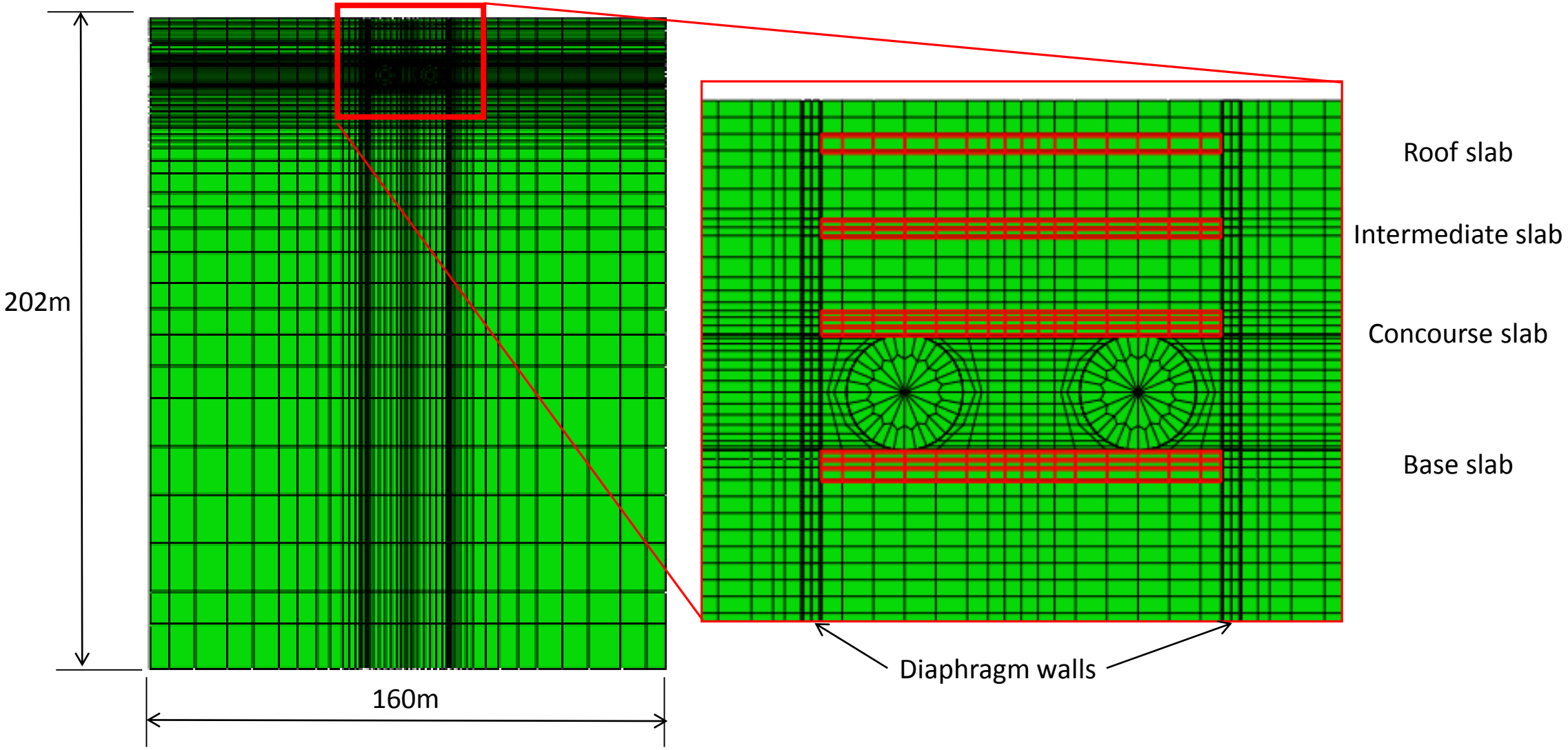
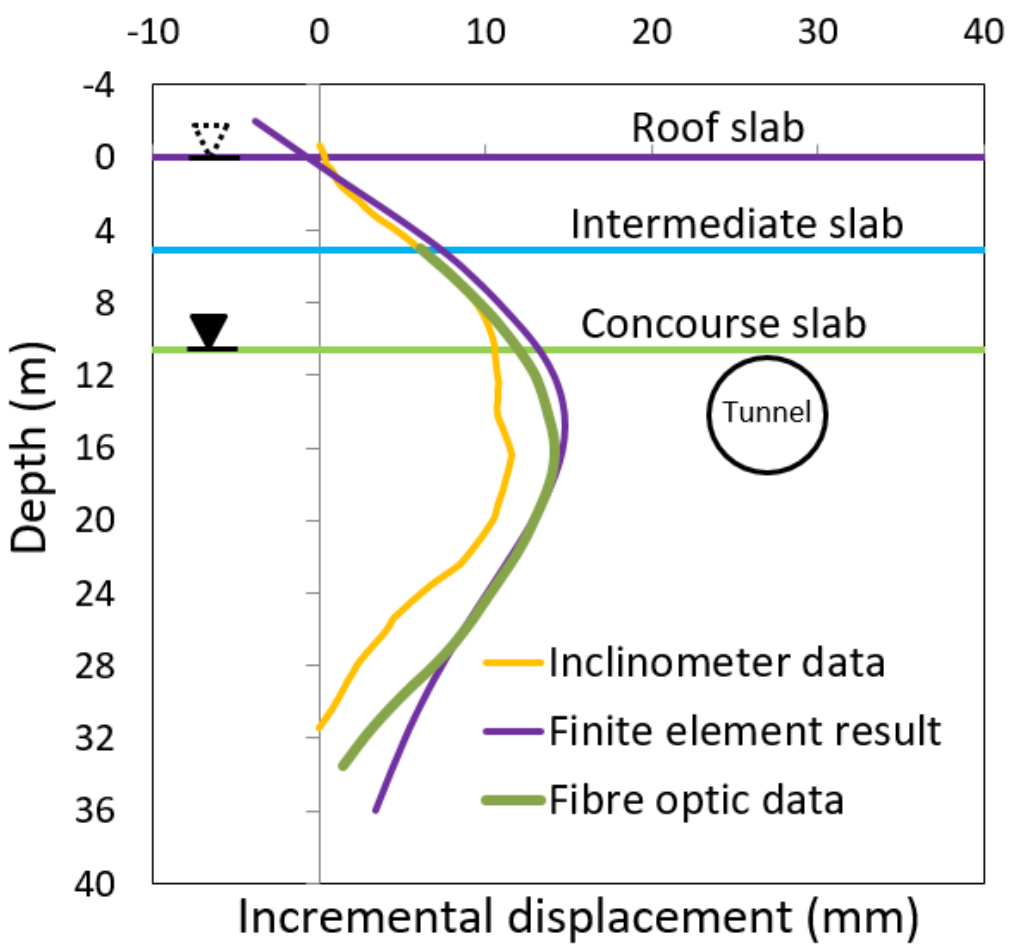


Figure 5

Click here to download Figure Figure 5.pptx



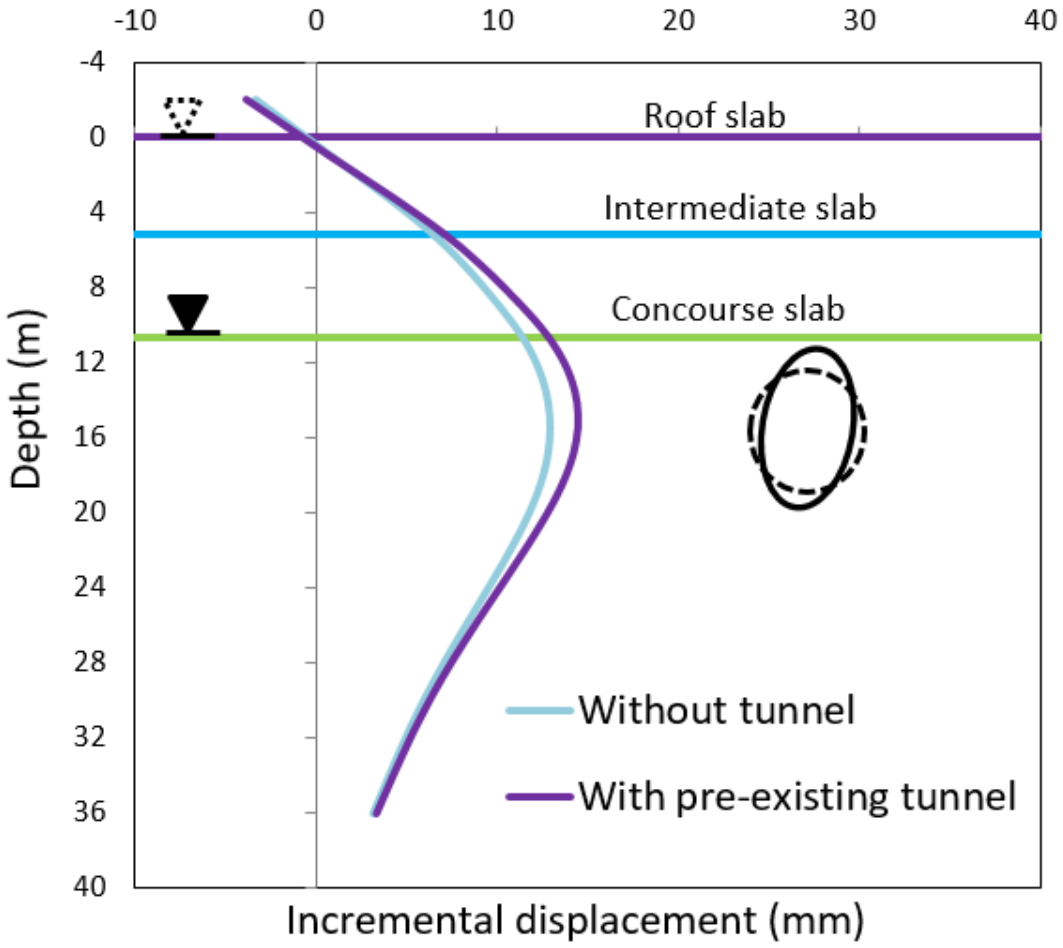
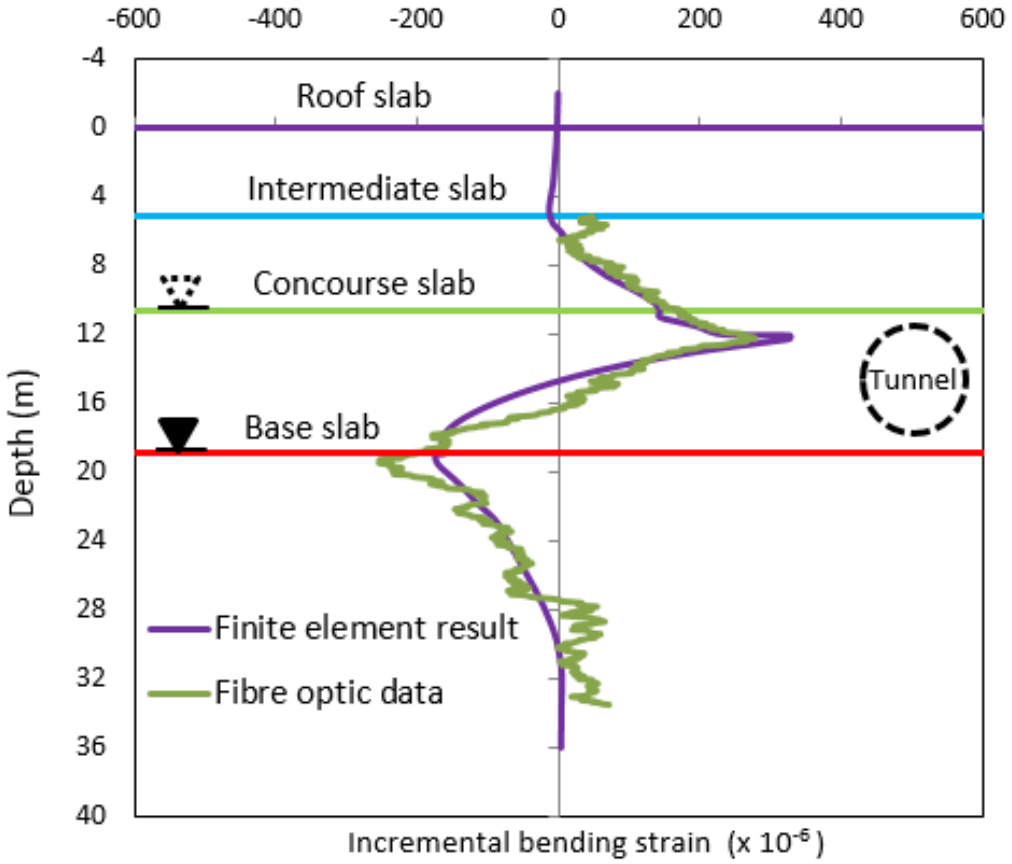
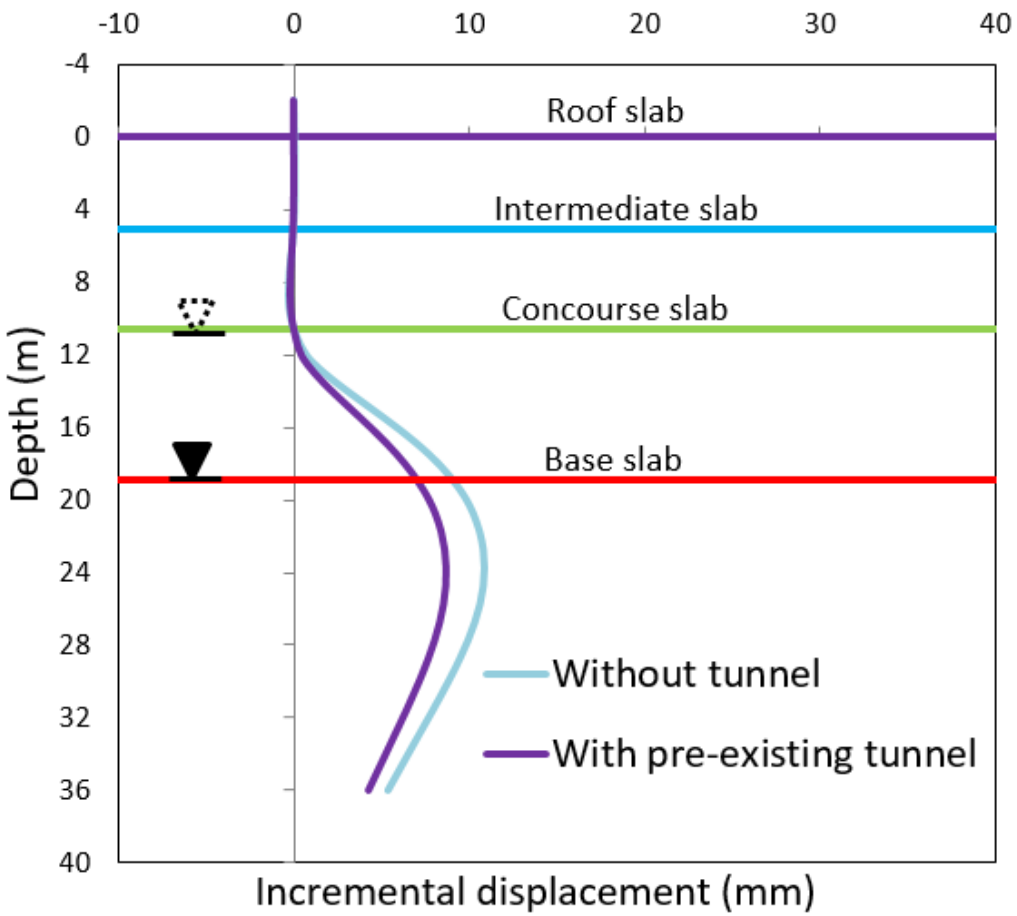


Figure 6

Click here to download Figure Figure 6.pptx





Table

Click here to download Table R3 Tables distributed fibre optic sensing.doc

Table 1 Soil properties for Made Ground and Terrace Ground (Crossrail Ltd., 2011 and 2015)

Stratum	Friction angle, ϕ' (°)	Young's Modulus, *E*' (MPa)	Poisson's ratio, *v*'	Coefficient of earth pressure at rest, K_0
Made Ground	25.0	5	0.2	0.6
Terrace Gravel	38.0	50	0.2	0.4

Table 2 Soil properties for London Clay and Lambeth Group (Laver, 2010)

Strata	M	e_0	u_1	m	C_b	ω_s	ρ_c	D	r	v'_{vh}	v'_{hv}	v'_{hh}	G_{hh}/G_{vh}	β_{vv}	β_{hh}	β_{vh}
London Clay	0.814	0.65	300	0.05	80	1	0.3	0.05	2	0.015	0.04	0.12	1.5	0.1	-0.05	0
Lambeth Group	1.07	0.65	100	0.1	900	50	0.37	0.05	2	0.2	0.2	0.2	1	0	0	0